



LAWRENCE
LIVERMORE
NATIONAL
LABORATORY

FY04 LDRD Final Report: Interaction of Viruses with Membranes and Soil Materials

C. M. Schaldach

February 10, 2005

Disclaimer

This document was prepared as an account of work sponsored by an agency of the United States Government. Neither the United States Government nor the University of California nor any of their employees, makes any warranty, express or implied, or assumes any legal liability or responsibility for the accuracy, completeness, or usefulness of any information, apparatus, product, or process disclosed, or represents that its use would not infringe privately owned rights. Reference herein to any specific commercial product, process, or service by trade name, trademark, manufacturer, or otherwise, does not necessarily constitute or imply its endorsement, recommendation, or favoring by the United States Government or the University of California. The views and opinions of authors expressed herein do not necessarily state or reflect those of the United States Government or the University of California, and shall not be used for advertising or product endorsement purposes.

This work was performed under the auspices of the U.S. Department of Energy by University of California, Lawrence Livermore National Laboratory under Contract W-7405-Eng-48.

Project Summary

Many outstanding and unsolved problems in water treatment involve the forces of attachment of organic species to membrane surfaces. These include fouling by natural organic matter, attachment of microbes to form biofilms, the attachment of viruses or retardation of viral transport near mineral surfaces and the unwanted transport of viruses through membrane pores. In all cases, solutions to these problems would benefit from a rigorous understanding of the physical basis for the interactions of the organic species with membrane surfaces. Understanding and quantifying the fundamental forces will improve our understanding of transport of viruses in the subsurface and may make it possible to design better methods for virus collection, detection and deactivation in water supplies, enhancing the vital role of water technology in national energy and environmental quality missions of the DOE and LLNL.

Although the scope of this project was very broad, we confined ourselves to simple virus-surface interactions for this 6-month project. By exploiting recent developments in proteomics which allow the downloading from public databases of atomistic-level information on the coordinates of amino acid residues in viruses for which the crystal structures have been resolved, we are able to account for the three-dimensional structure of the virus, advancing the state-of-the-art in viral-surface interactions.

Accomplishments: We exceeded our expected results, investigating several bacterial (MS2, Q β), animal (Foot-and-Mouth) and human (Dengue, Hepatitis B, Human rhinovirus-16, Norwalk) viruses in addition to the proposed plant virus (Cowpea Mosaic Virus). (See section entitled "Viruses of National Importance"). We have submitted one manuscript for publication, are preparing a second, and have presented our work (poster) at an American Geophysical Union meeting.

Environmental field studies use bacteriophages (viruses which infect bacteria) and non-pathogenic human viruses to study aspects of viral transport in ground water. For comparison, we investigated three of those same environmentally-relevant viruses, MS2, Q β and Norwalk; the first set of calculations and results, describing the influence of ionic strength on the electrostatic interactions of these viruses with surfaces, has been submitted for publication in the *Journal of Colloid and Interface Science*. The Abstract is included below and the full paper is attached to this report; it contains the details of the method of calculation and results of those calculations. The remainder of this report describes our extension of the initial virus-surface model to the calculation of binding energies of viruses to surfaces; this work is included in a second manuscript currently in preparation. We also presented a poster at the American Geophysical Union (AGU) Fall Meeting in San Francisco, CA in December 2004.

Our investigations during this project have provided a mechanism to explain many environmental studies which have shown that electrostatic interactions play a dominant role in viral adsorption to mineral surfaces, dependent upon the pH and ionic strength of the aqueous environment, as well as the type of virus. Most importantly, for the first time, the role of the spatial distribution of amino acids in the viral coat was found to explain the observations. Experimental evidence further suggests that such forces might also be responsible for deactivation of viruses, although a detailed mechanism has not been put forth. With the successful completion of this project, we are now in a position to address

the question of virus deactivation and use that understanding to design materials which would optimize the collection and deactivation of viruses.

Abstract (First Paper)

The influence of ionic strength on the electrostatic interaction of viruses with environmentally relevant surfaces was determined for three viruses, MS2, Q β and Norwalk. The environmental surface is modeled as charged Gouy-Chapman plane with and without a finite atomistic region (patch) of opposite charge. The virus is modeled as a particle comprised of ionizable amino acid residues in a shell surrounding a spherical RNA core of negative charge, these charges being compensated for by a Coulomb screening due to intercalated ions. Surface potential calculations for each of the viruses show excellent agreement with electrophoretic mobility and zeta potential measurements as a function of pH. The results indicate that the electrostatic interaction between the virus and the planar surface, mitigated by the ionic strength of the solute, is dependent upon the spatial distribution of the amino acid residues in the different viruses. Specifically, the order of interaction energies with the patch (MS2 greatest at 5 mM; Norwalk greatest at 20 mM) is dependent upon the ionic strength of the fluid as a direct result of the viral coat amino acid distributions.

Abstract (Virus-Surface Model extended)

We have developed an atomistic-scale method of calculation of the binding energy of viruses to surfaces including electrostatic, van der Waals, electron-overlap repulsion, surface charge polarization (images), and hydrophobic effects. The surface is treated as a Gouy-Chapman plane allowing inclusion of pH and ionic strength effects on the electrostatic potential at each amino acid charge. Van der Waals parameters are obtained from the DREIDING force field and from Hamaker constant measurements. We applied this method to the calculation of the Cowpea Mosaic Virus (CPMV), a negatively charged virus at a pH of 7.0, and find that the viral-gold surface interaction is very long range for both signs of surface potential, a result due to the electrostatic forces. For a negative (Au) surface potential of -0.05 volts, a nearly 4 eV barrier must be overcome to reach 1 nm from the surface.

Method of Calculation

The virus is treated as a protein shell surrounding a spherical core of negative charge (RNA or DNA). The amino acid locations and types which comprise the shell are obtained from the RCSB Protein Data Bank (1) and the spherical core (for CPMV, this consists of 5889 nucleotides) is discretized into elements (2). The electrostatic charge on the individual amino acids is obtained as a function of fluid pH (3), a procedure which has been shown to give rise to viral zeta potentials in excellent agreement with experiment (2). We employ a rigid virus framework: The atoms comprising the virus are held immobile in these configurations.

The surface to which we are binding the viral particle is modeled as an infinite charged plane, the source of electrostatic potentials and fields which have been obtained by Gouy and Chapman (4) by solving the non-linear linear Poisson-Boltzmann equation. At close

distances of interaction of the virus with the surface, van der Waals and electron-electron repulsive forces must be included.

Beginning with the electronic structure of an atom, we ultimately obtain the viral surface interaction through several steps, each of which increases the scale. That is, we first obtain amino acid constituent atom (C, H, O, N, S) interactions with a surface (Au) atom, then integrate over the infinite planar surface to obtain amino acid atom interactions with a gold surface. We next calculate the optimized geometry for all 20 amino acids at the 6-31G** level of theory using GAMESS (6). These atomic coordinates of each amino acid are employed to obtain the individual amino acid interactions, both van der Waals and electron-electron repulsion, with the gold surface. Finally, the amino acids are aggregated into the protein shell to obtain the total electrostatic, van der Waals, and electron-electron repulsion of the virus with the material surface.

In Fig. 1, the pairwise atom-atom interactions between the constituents of the amino acids and the atoms of the material surface are presented. Electron-electron repulsive energies are obtained by local density functional methods (7) which involve solving the Schrödinger equation for the individual atoms and then obtaining the interaction between the atoms including increased kinetic and correlation energy in the overlap region between them. The method applies to interactions such as between rare gases where covalent effects, electron transfer, can be neglected.

The attractive pairwise van der Waals interaction at separation, r_{ij} , between each of the atoms, $i=(C, O, N, H, S)$, in the amino acid residues comprising the viral coat proteins and a gold atom, $j=(Au)$, is obtained using the DREIDING force field (8)

$$W_{ij}^{vdw} = -\frac{2D_{ij}^0}{\rho_{ij}^6} \quad (1)$$

where $\rho_{ij} = r_{ij} / r_{ij}^0$. D_{ij}^0 and r_{ij}^0 are obtained using the geometric means

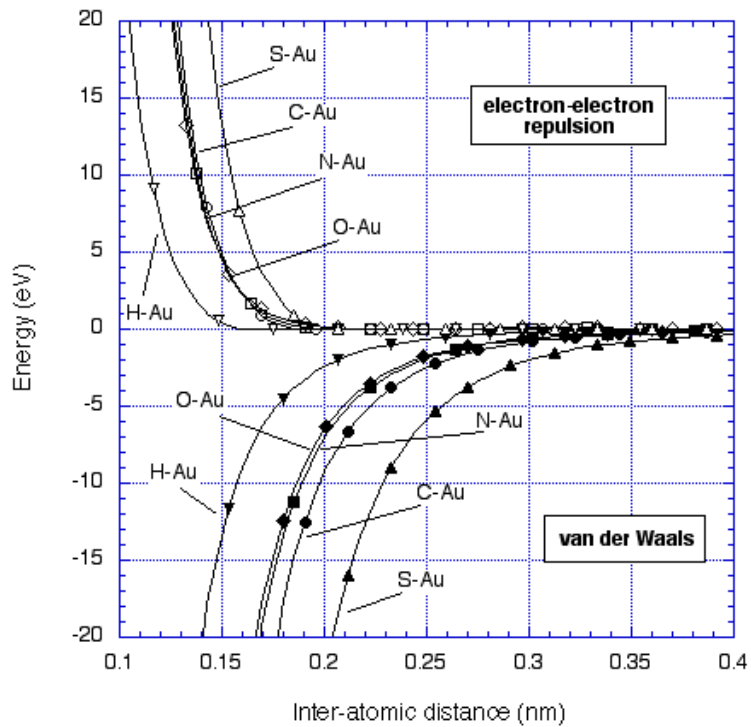


Figure 1. Pairwise atom-atom interactions between the constituents of the amino acids and the atoms of the material surface.

and

$$D_{ij}^o = (D_{ii}^0 D_{jj}^0)^{\frac{1}{2}} \quad (2)$$

$$r_{ij}^o = (r_{ii}^0 r_{jj}^0)^{\frac{1}{2}}$$

The parameters D_{ii}^0 and r_{ii}^o for C, O, N, H, S are from DREIDING and are reproduced for convenience in Table I along with the parameters involving Au which were obtained from recent AFM experiments (9) as described below.

The interaction of an atom at distance, D, from an infinite surface having atomic number density, ρ (atoms/cm³) is given by

$$W_{surf}^i = \int_D \rho w^i dV = 2\pi \int_D dz \int_0^\infty w^i x dx \quad (3)$$

where w^i is either the van der Waals energy per atom (i=1) or the electron-electron repulsive energy per atom (i=2). In Eq. 3, the z-axis is normal to the surface. In the i=1 case, $w^1 = -C/r^6 = -C/(x^2 + z^2)^3$ resulting in the analytic expression (5),

$$W_{surf}^1 = -\frac{\pi C \rho}{6D^3} \quad (4)$$

Similarly, the electron-electron repulsive interaction (i=2) of each of the amino acid atoms with the gold surface is obtained. Here, there is no simple analytic expression for the energy per atom; we perform the integration indicated in Eq. 3 numerically using splines to interpolate between directly calculated points.

The DREIDING force field does not contain parameters for gold. However, recent atomic force microscopy (AFM) experiments by Ashby, et al (9) resulted in a Hamaker constant for gold-gold interactions of 1×10^{-19} J. If the AFM tip is considered to be a sphere of radius R comprised of gold atoms having atom number density, r , an integration over the sphere as well as the flat infinite surface can be performed, leading to an expression for the sphere-surface interaction,

$$W_{surf}^{sphere} = -\frac{\pi^2 \rho^2 C}{6} \left(\frac{R}{D} \right) = -\frac{AR}{6D} \quad (5)$$

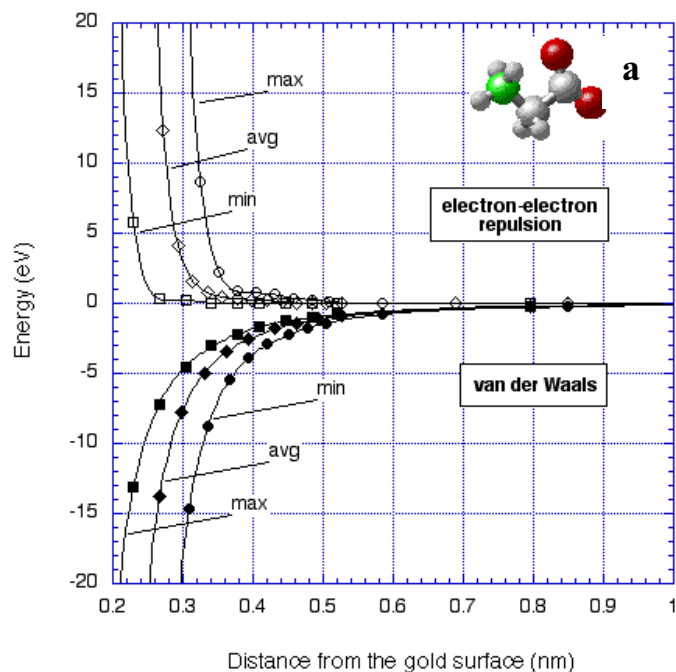
where $C (= -2D_{ii}^0 r_{ii}^0)$ is the pairwise Au-Au van der Waals interaction parameter (see Table I) and A is the measured Hamaker constant.

Table I. Van der Waals parameters for C, H, O, N, S are from DREIDING (8) (see Eqs. 1-2) and for Au from Ashby, et al (9) (see text).

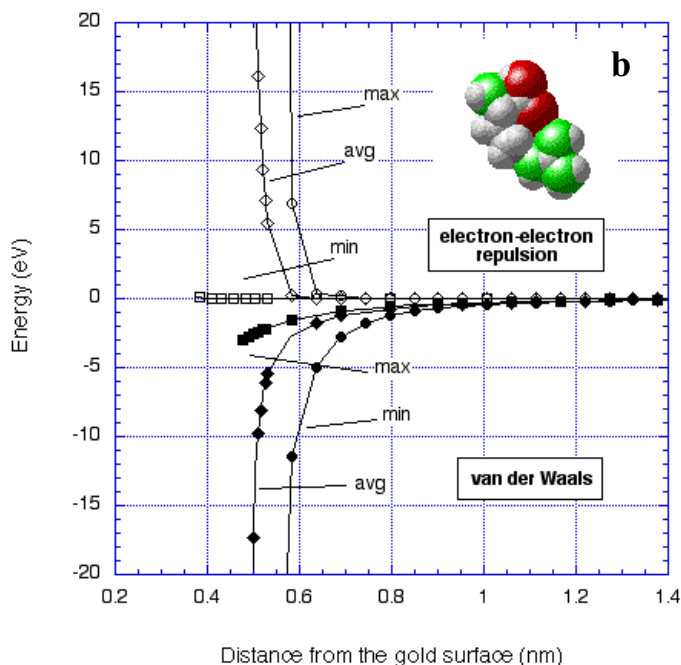
Atom	D_{ij}^0 (kcal/mol)	r_{ij}^0 (Å)
C	0.0951	3.8983
H	0.0152	3.1950
O	0.0957	3.4046
N	0.0774	3.6621
S	0.3440	4.0300
Au	0.0550	4.0730

At this point, we have the interactions of individual amino acid atoms with the infinite surface. We next calculated the properties of each of the 20 amino acids comprising the viral coat quantum mechanically using GAMESS, optimizing the geometry using 6-31G** wavefunctions. Each of the molecules so formed is brought down on the gold surface in steps of 0.05 nm from $0 < r < 20$ nm where r is the centroid of the amino acid residue, whose atoms are held fixed in their pre-determined minimum energy configurations. At each distance step, the amino acid molecule is rotated about each of the x, y and z axes in steps of one degree, and the maximum, minimum and average electron-electron repulsion and van der Waals energies recorded. In this way, we have

estimated bounds for the interaction of each amino acid with the surface.



In Fig. 2, we present representative results of these calculations for a) glycine (spherical), b) arginine (longitudinal), and c) cysteine (contains sulfur). The first two were chosen because of their widely differing geometries and the third because it contains sulfur which is well known to have a strong van der Waals interaction (see Table I). It is first of all to noted from Fig. 2 that, as a consequence of its geometry, glycine approaches nearer the gold surface than arginine or cysteine before its electron-electron repulsion exponentially prevents it. For example, the maximum repulsive energy crosses an arbitrary 5 eV threshold for glycine at 0.35 nm, arginine at 0.6 nm and cysteine at 0.45 nm. Arginine (Fig. 2b), being highly linear, contains atoms which experience this (maximum) repulsion when its centroid is at much greater distances from the surface (its axis being parallel to the normal to the surface); cysteine represents an intermediate case in this respect. When the axis of this linear molecule is parallel to the surface,



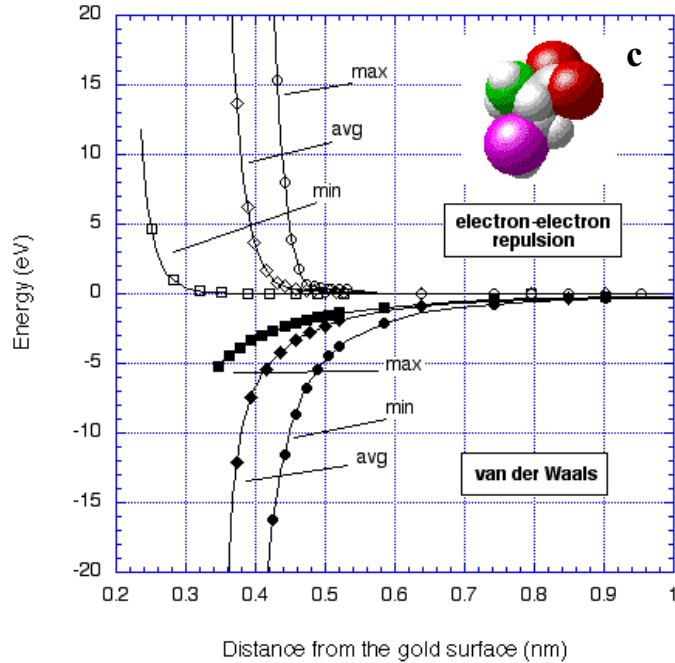


Figure 2. Interactions of individual amino acids with an infinite gold surface. a) glycine; b) arginine; c) cysteine.

the molecule can approach very close to the surface before it experiences electron-electron repulsion. Cysteine is also quite linear and behaves similarly (Fig. 2c) with regard to being able to approach near the gold surface without being repelled. The difference in the distance at which the 5eV arbitrary repulsive threshold is crossed for the maximum and minimum configurations is least for glycine and greatest for arginine.

As might be expected, in all cases, when the electron-electron repulsion is greatest, the van der Waals attraction is the least (most negative) and when the electron-electron repulsion is least, the van der Waals attraction is greatest

(least negative). Within the rigid virus framework employed here, this suggests choosing a) Method I: maximum repulsion and minimum van der Waals curves for each amino acid; b) Method II: minimum repulsion and maximum van der Waals curves for each amino acid; and c) Method III: the average repulsive and van der Waals curves for each amino acid in estimating the effect of these interactions on the binding of the virus to the surface.

Results

In Fig. 3, we have plotted the total energy of the CPMV as a function of distance from the surface, each point having been obtained as the minimum energy as the viral particle is rotated about the x, y and z axes through the centroid. The calculations are performed for Methods I, II and III for surface potentials of ± 0.05 volts and for an ionic strength of 10 mM NaCl at pH 7.0 at which pH the zeta potential of the CPMV is negative. It is first of all to be noted that the interaction is very long range for both signs of

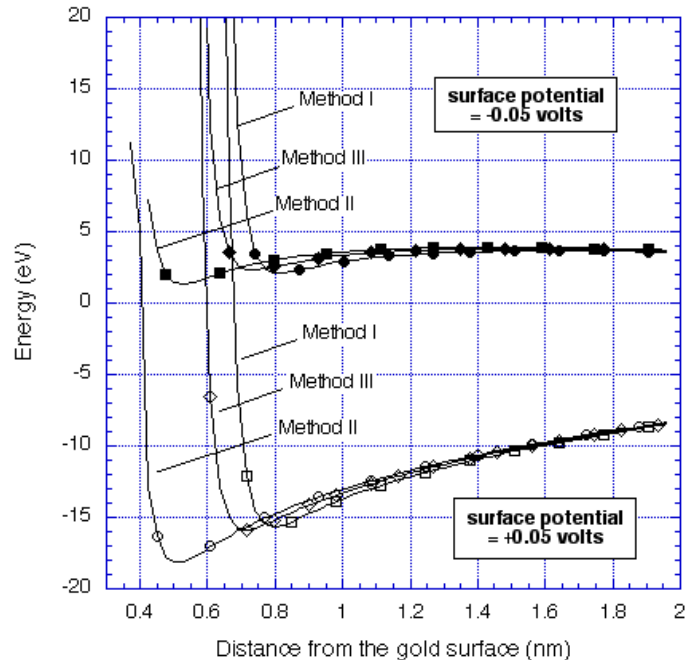


Figure 3. Total binding energy of the Cowpea Mosaic Virus (CPMV) to a gold surface.

surface potential, a result due, as we shall see, to the electrostatic forces. For all three methods, the negative surface potential results in a repulsive viral interaction at all distances of approach; for the parameters chosen for Fig. 3, a nearly 4 eV barrier must be overcome to reach 1 nm from the surface. At these short viral-surface distances, Methods I, II and III produce somewhat different structures having local minima at 0.52, 0.75 and 0.81 nm, respectively. The positive surface potential in Fig 3 gives rise to long-range attraction of the CPMV. Again, the choice of short-range forces (Methods I-III) affects the location of the minima below 1 nm.

The components of the energy for the -0.05 volt surface potential are shown in Figure 4 over a longer range of distances than Fig. 3. From this figure, it is clear that the electrostatic component dominates the energy for long distances. As the CPMV is moved away from the surface, the total energy goes to zero at 14 nm. At short distances, the total energy has a maximum of 3.7 eV at 1.5 nm from the surface. At distances < 1.5 nm, the van der Waals begins to dominate until the virus is approximately 0.75 nm from the surface. At this close distance, the electron-overlap repels the virus and prevents it from crashing into the gold surface.

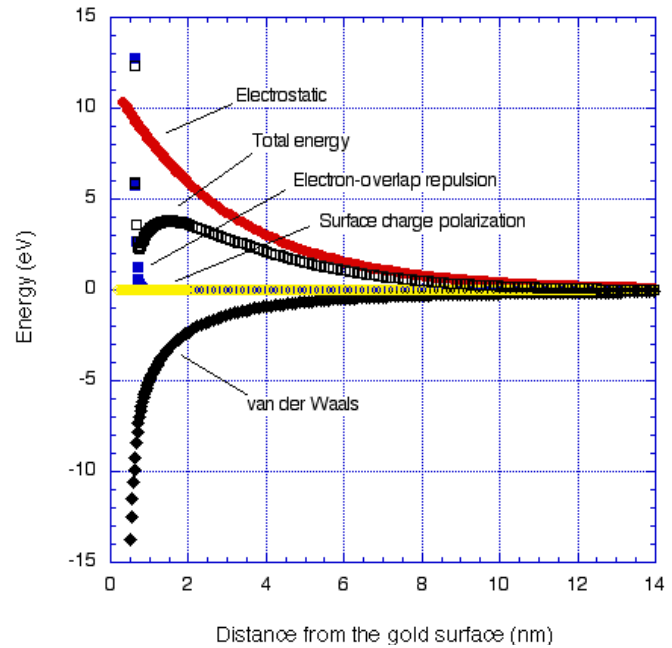
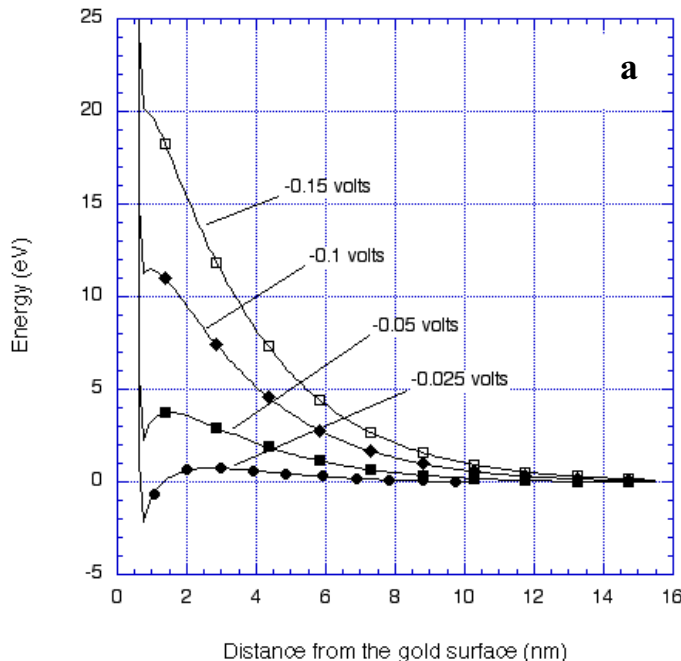


Figure 4. Components of the binding energy of the CPMV to a gold surface with a surface potential of -0.05

distance, the electron-overlap repels the virus and prevents it from crashing into the gold surface.



We varied the electrostatic potential applied to the gold surface and the resulting CPMV binding energies and forces are shown in Figure 5. As can be seen in Fig. 5a, a surface potential of -0.025 volts results in an energy barrier of 0.74 eV at a viral-surface distance of 2.6 nm, before binding with a total energy of -2.2 eV. With larger potentials (-0.05 , -0.1 , -0.15), the energy barriers are considerably higher (3.7, 11.5, 20.1, respectively).

The corresponding forces are plotted in Fig. 5b. Note the agreement between the

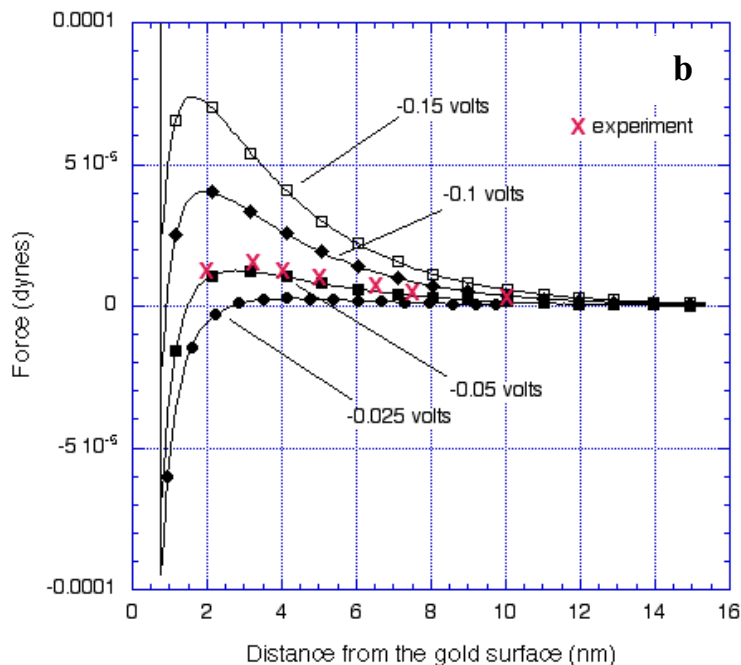


Figure 5. a) Calculated binding energies of and b) forces on the CPMV, as a function of surface potential.

experimentally (Atomic Force Microscopy) determined forces and the calculation for a surface potential of -0.05 volts, providing a validation of our methods.

Viruses are the smallest of biological pathogens which need to be removed from ground water. Membranes consisting of ~ 100 nm-diameter holes might serve such a purpose. We have developed a method of calculation of the electric fields in the vicinity of such membranes (10) which, together with the viral models developed here, form the basis for understanding

how viruses might be manipulated by nanostructures.

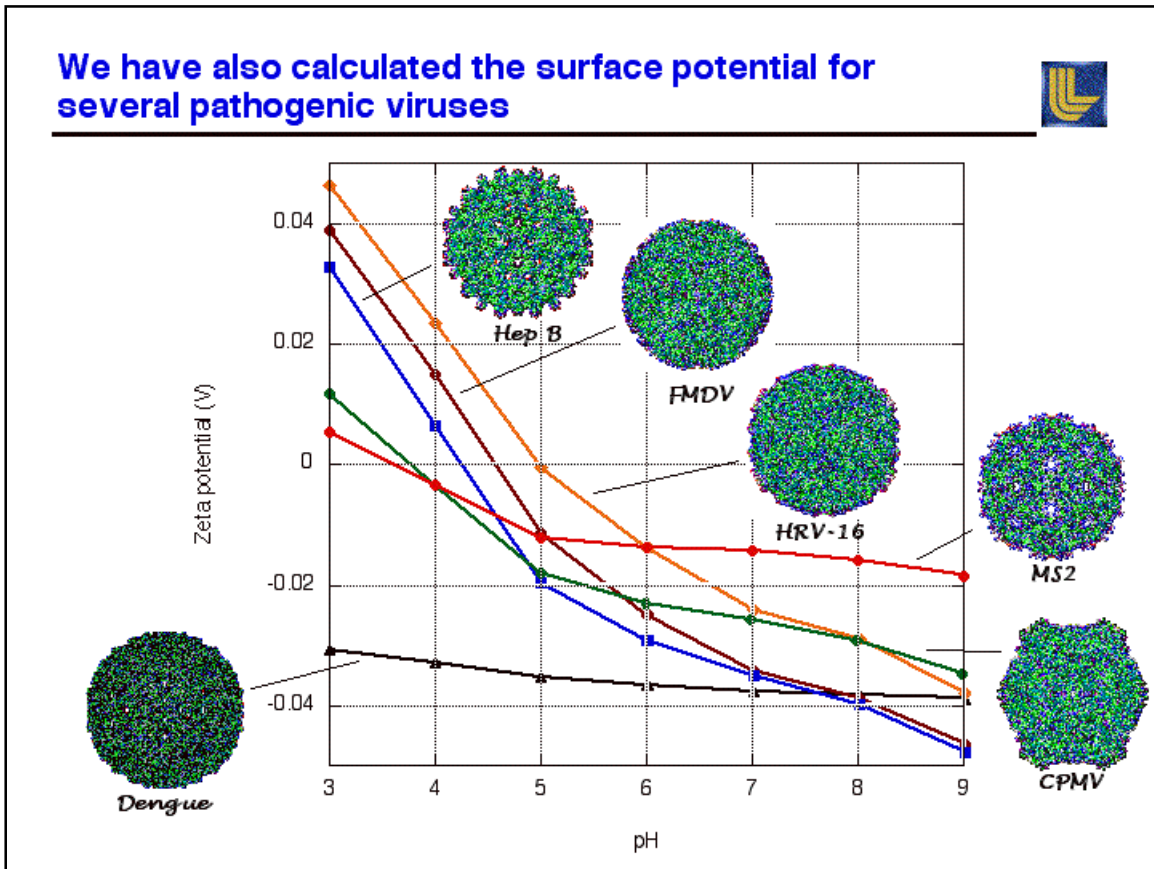
Viruses of National Importance

We investigated several viruses with national security or health implications. These viruses are summarized in Table II.

Table II. Summary of viruses with national security and health implications (11-15).

Virus	PDB #	Brief description of disease
Dengue	1K4R	Human, hemorrhagic fever
Foot-and-Mouth (FMD)	1QQP	Animal, economic devastation
Hepatitis B (HepB)	1QGT	Human, cirrhosis and liver cancer
Human Rhinovirus-16 (HRV-16)	1AYM	Human, common cold
Norwalk	1IHM	Human, gastroenteritis

We calculated the zeta potential for each of these viruses, and show the results combined with the amino acid representations for several of them in the figure below; MS2 and CPMV are provided for comparison purposes. The zeta potential is a measure of the



surface charge on the viral particle, an important aspect of the viral-surface interaction. The viral surface charge is a critical parameter in understanding the use of surrogates (e.g., MS2) for the other pathogenic viruses in ground water filtration. It is interesting that Hepatitis B, Foot-and-Mouth and Human Rhinovirus-16 have similar shaped curves, indicating significant changes in viral surface charge and surface interaction with small changes in pH. This gradient is to be compared to the zeta potential for MS2, which remains constant over the pH range of 5.0-8.0. MS2 is the usual surrogate for human pathogens. The CPMV is similar to MS2 at pH < 5.0, but the CPMV does become more negatively charged at the higher pHs. Note that the point of zero charge for nearly all of these viruses ranges from pH 3.5 (MS2) to pH 5.0 (HRV-16). Only the Dengue virus does not have a point of zero charge within this range of environmentally-relevant pHs. Therefore, under most environmental conditions, these viruses will be negatively charged in the ground water.

References

1. <http://www.rcsb.org/pdb/> For the Cowpea Mosaic Virus, the access key is 1NY7.
2. Schaldach, C.M., Bourcier, W.L., Shaw, H.F., Viani, B.E., Wilson, W.D., “The influence of ionic strength on the interaction of viruses with charged surfaces under environmental conditions”, *J. Colloid Interface Sci.*, submitted.
3. Stryer, L., *Biochemistry*; 4th Ed., W.H. Freeman and Co., New York, 1995.
4. Gouy, G., *J. Physique* **9** (1910) 457; also, independently, Chapman, D.L., *Phil. Mag.* **25** (1913) 475.
5. Israelachvili, J., *Intermolecular and Surface Forces*; 2nd Ed., Academic Press, San Diego, 1992.
6. Schmidt, M.W., Baldridge, K.K., Boatz, J.A., et al, “General Atomic and Molecular Electronic Structure System”, *J. Comput. Chem.* **14** (1993) 1347.
7. Wilson, W.D., Schaldach, C.M., “Adsorption of Molecules on a Charged Polarizable Surface in an Electrolyte”, *J. Colloid Interface Sci.* **208** (1998) 546; Wilson, W. D., and Bisson, C.L., *Phys. Rev. B* **3** (1971) 3984. A similar method was independently introduced by Gordon, R. G., and Kim, Y. S., *J. Chem. Phys.* **56** (1972) 3122.
8. Mayo, S.L., Olafson, B.D., Goddard, W.A. III, “DREIDING: a generic force field for molecular simulations”, *J. Phys. Chem.* **94** (1990) 8897.
9. Ashby, P.D., Chen, L., Lieber, C.M., “Probing Intermolecular Forces and Potentials with Magnetic Feedback Chemical Force Microscopy”, *J. Am. Chem. Soc.* **122** (2000) 9467.
10. Schaldach, C.M., Bourcier, W.L., Paul, P.H., Wilson, W.D., “Electrostatic Potentials and Fields in the Vicinity of Engineered Nanostructures”, *J. Colloid Interface Sci.* **999** (2004) 9999.
11. Kuhn, R.J, Zhang, W., Rossmann, M.G., et al, “Structure of Dengue Virus: Implications for Flavivirus Organization, Maturation, and Fusion”, *Cell* **108** (2002) 717.
12. Fry, E.E., Lea, S.M., Jackson, T., et al, “The Structure and Function of a Foot-and-Mouth Disease Virus—Oligosaccharide Receptor Complex”, *EMBO J.* **18** (1999) 543.
13. Wynne, S.A., Crowther, R.A., Leslie, A.G.W., “The Crystal Structure of the Human Hepatitis B Virus Capsid”, *Molecular Cell* **3** (1999) 771.
14. Hadfield, A.T., Lee, W., Zhao, R., et al, “The Refined Structure of Human Rhinovirus 16 at 2.15 Å resolution: Implications for the Viral Life”, *Structure* **5** (1997) 427.
15. Prasad, B.V.V., Hardy, M.E., Dokland, T., et al, “X-ray Crystallographic Structure of the Norwalk Virus Capsid”, *Science* **286** (1999) 287.